INL/CON-18-44482-Revision-1

Grain Boundary Characteristics of SiC in Irradiated, AGR-2 TRISO Particles

T. M. Lillo, Subhashish Meher, I. J. van Rooyen

October 2018

The INL is a U.S. Department of Energy National Laboratory
operated by Battelle Energy Alliance

INL/CON-18-44482-Revision-1

Grain Boundary Characteristics of SiC in Irradiated, AGR-2 TRISO Particles

T. M. Lillo, Subhashish Meher, I. J. van Rooyen

October 2018

Idaho National Laboratory
Idaho Falls, Idaho 83415

http://www.inl.gov

Prepared for the
U.S. Department of Energy

Under DOE Idaho Operations Office
Contract DE-AC07-05ID14517

Proceedings of HTR 2018
Warsaw, Poland, October 8-10, 2018
Paper HTR 2018-3025

GRAIN BOUNDARY CHARACTERISTICS OF SIC IN IRRADIATED, AGR-2 TRISO PARTICLES

T. M. Lillo[1], I. J. van Rooyen[2] and S. Meher[1]
Idaho National Laboratory
Idaho Falls, ID 83415-2211, USA
phone: +1-208-5269746, thomas.lillo@inl.gov

[1] Materials Science and Engineering Department, Idaho National Laboratory, PO Box 1625, Idaho Falls, Idaho 83415-2211, USA

[2] Fuel Design and Development Department, Idaho National Laboratory, PO Box 1625, Idaho Falls, Idaho 83415-6188, USA

Abstract – *Microstructural characterization of the SiC layer was carried out on neutron-irradiated, tristructural isotropic (TRISO)-coated fuel particles from the Advanced Gas Reactor (AGR)-2 experiment. The SiC grain-boundary distribution in each particle was characterized with precession electron diffraction in the transmission electron microscope. Generally, the distributions in the AGR-2 TRISO particles (fabricated at the pilot scale by an industrial vendor) were similar to the Variant 3, AGR-1 TRISO particles made at laboratory scale at Oak Ridge National Laboratory. In the two AGR-2 particles examined, there were slightly more random, high-angle grain boundaries, in conjunction with slightly fewer low-angle grain boundaries compared to AGR-1 TRISO particles previously examined. Plotting the Ag-110m retention exhibited by both Variant 3 AGR-1 and AGR-2 irradiated TRISO particles against various grain boundary types revealed that Ag retention directly correlates with the random, high-angle and inversely with twin grain-boundary fraction in the center area of the SiC layer. Observations associated with localized areas of precipitation also will be reported in this paper.*

I. INTRODUCTION

The silicon carbide (SiC) layer of tristructural isotropic (TRISO)-coated particle fuel for advanced, high-temperature nuclear reactors acts as the primary barrier for containment of fission products. TRISO fuel with uranium carbide/uranium oxide (UCO) fuel kernels for high temperature gas-cooled reactors is currently undergoing testing and characterization under the Advanced Reactor Technology fuel qualification program, sponsored by US Department of Energy–Office of Nuclear Energy. Previously, TRISO-coated fuel, produced on a laboratory scale at Oak Ridge National Laboratory and irradiated in the Advanced Gas Reactor Experiment-1 (AGR-1) in the Advanced Test Reactor (ATR) at Idaho National Laboratory (INL), has been characterized using advanced microscopy techniques [1-5]. A similar advanced microstructural characterization study of the SiC layer on TRISO-coated fuel, produced at pilot scale by an industrial vendor and irradiated in the AGR-2 experiment in ATR at INL, was performed to compare the behavior of pilot-scale fuel as part of the fuel upscale project for qualification. Further understanding of fission-product behavior within TRISO layers, especially of Ag-110m (due to its high mobility in intact TRISO layers), in the SiC layer during neutron irradiation is also explored. The results reported in this study concern one as-irradiated TRISO particle, AGR2-223-RS06 and one irradiated TRISO particle that had been subjected to safety testing at 1600°C for 300 h, AGR2-222-RS36. (Safety testing was performed to understand fission-product release behavior during off-normal operating conditions). This work will be expanded at a later stage to include other particles from the AGR-2 experiment.

II. EXPERIMENTAL PROCEDURE

The AGR-2 TRISO fuel particles examined in this study were fabricated at BWX Technologies, using coating conditions similar to those used to

produce Variant 3 TRISO-coated fuel particles for the AGR-1 experiment [6]. The TRISO particles were overcoated and compacted into cylinders at ORNL and irradiated in the ATR at INL.

The irradiation conditions for the *compacts* from which these particles were taken, are summarized in Table 1. (Additional information on the AGR-2 experiment and irradiation conditions can be found in [7].) The fractional retention of Ag-110m is determined by the ratio of measured Ag-110m content to the value predicted from physics calculations [8]. Both particles exhibited extensive release of their predicted Ag-110m inventory.

Table 1: TRSIO particle characteristics and average compact irradiation conditions. [7]

Particle ID	Ag-110m Retention[a] %	Burnup[b], % FIMA	Neutron Fluence[c], $\times 10^{25}$ n/m^2	TAVA[b], °C
AGR2-222-RS36	8[d]	12.6	3.39	1287
AGR2-223-RS06	BLD[e]	12.7	3.46	1296

[a] Estimates of Ag retention are based on the measured inventory divided by the predicted inventory.
[b] Average values associated with the fuel compact: individual particle conditions may differ significantly.
[c] E >0.18 MeV
[d] After safety testing, 1600°C, 300 hrs
[e] Below the limits of detection

Transmission electron microscopy (TEM) samples from the SiC layer of each particle, which was about 35 µm thick, were produced from a polished cross section of each particle using standard focused ion beam (FIB) techniques. Fig. 1a shows the polished cross section of particle AGR2-222-RS36 while Fig. 1b shows the cross section of particle AGR2-223-RS06. In this cross section view, both particles exhibit a partial delamination between the buffer and IPyC layers (a common feature in AGR TRISO fuel after irradiation), but the IPyC/SiC interface appears to remain bonded in both particles, at least in these cross sections. General areas where samples were taken from the SiC layer of both particles are shown in Fig. 1, and two locations on each particle were analyzed: one in the vicinity of the delamination (Location A) and one where the buffer/IPyC interface appears to be intact (Location B). TEM lamellae were extracted from inner, center, and outer regions of the SiC layer on each particle.

Grain boundary distributions within the SiC layer were determined using SiC grain orientation information gathered from precession electron diffraction (PED) TEM data (Tecnai TF30-FEG STwin, operating at 300 kV, at the Center for Advanced Energy Studies) using the ASTAR system (NanoMegas, Inc.). An electron probe size of 5 nm, in conjunction with a 4-nm step size, was used to collect crystallographic orientation data. The crystallographic information was exported and analyzed using EDAX OIM v7.1.0 software. Two data cleanup routines (see [2] for details) were applied to all data and resulted in less than 3% of the data points being affected, well below the limit of 10% allowed in Section 12.2 of American Society for Testing and Materials Standard E2627 [9]. Grain boundaries were defined for a misorientation equal to or greater than 2 degrees. The range of coincident site lattice (CSL)-related grain boundaries was defined to include Σ3 through Σ29.

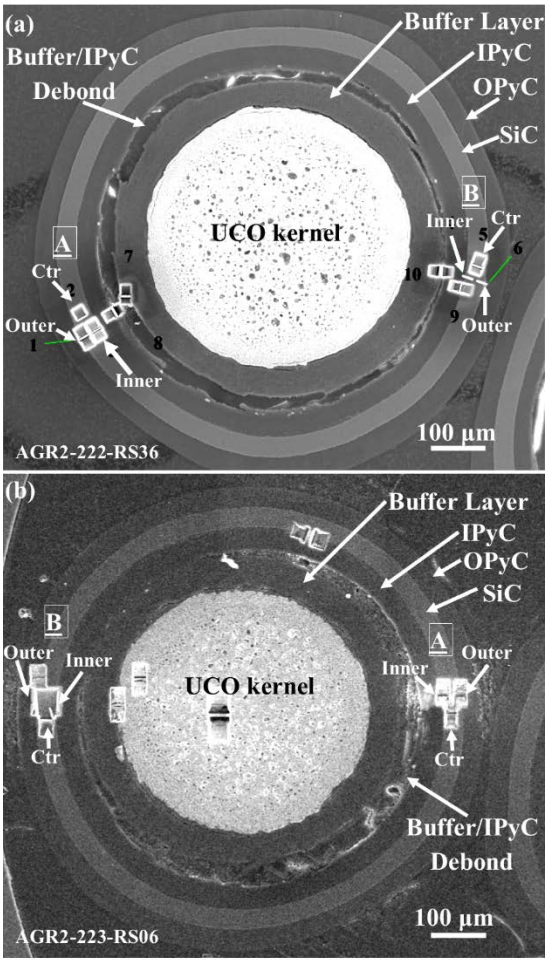

Fig. 1: SEM images of the cross section through particles (a) AGR2-222-RS36 and (b) AGR2-223-RS06 with the locations of analysis shown.

Three areas on the inner, center, and outer samples from each location and particle were analyzed. The standard error in the grain boundary

distributions was determined by dividing the standard deviation for each measured value of grain-boundary type (low angle, random high angle, CSL value or misorientation angle) by the square root of the number of areas analyzed, i.e., the number of observations, to yield the standard error, which has been used for the error bars in the plots that follow.

Additionally, in each area, fission-product precipitates were analyzed using energy dispersive x-ray spectroscopy (EDS) to obtain qualitative information of fission products and transuranic elements in the precipitates. The precipitates associated with grain boundaries were then correlated with parameters associated with the grain boundary using the PED data.

III. RESULTS

III.A. AGR2-222-RS36—Comparison of Grain Boundary Distributions in Locations A & B

The grain-boundary distributions associated with inner, center, and outer regions of the SiC layer at Locations A and B are shown in Fig. 2. Generally, there is no statistical difference in the distributions across the SiC layer with a notable exception in the twin fraction in the inner region of the SiC layer at Location B (see, especially Fig. 2b for Σ3 boundaries). The twin fraction here is lower than in other areas of Location B, e.g., the center and outer regions, and considerably lower than in all areas at Location A. Additionally, Fig. 2c indicates a higher fraction of low-angle grain boundaries at Location B throughout the SiC layer than at Location A. The potential for deformation of the SiC layer at Location B during irradiation, and the generation of low-angle grain boundaries, seems unlikely. However, it may be a possible explanation since the time-averaged, volume averaged temperature (TAVA) of this compact was $>0.5T_{MP,SiC}$ (and the actual particle temperature may be considerably higher [10]), the SiC layer experienced considerable neutron fluence, which can enhance diffusional creep and the buffer/inner pyrolytic carbon (IPyC) layers remained bonded at Location B potentially giving rise to an asymmetrical stress distribution in the SiC layer. However, the main conclusion from the grain-boundary distribution data is that although the distributions are generally the same at both location, there can be considerable variation with position, i.e., within the inner, center, or outer SiC layer, as well as from location-to-location. The variation is expected to result from the chemical vapor deposition (CVD) SiC-layer fabrication process in a fluidized bed reactor in which local SiC deposition conditions can be expected to vary as a function of time and position in the furnace.

Analysis of fission-product precipitates by EDS showed most of the precipitates contained Pd and, most often, only Pd (Fig. 3a). These Pd-containing precipitates were found throughout the SiC layer at both Locations A and B. Very few Ag-containing precipitates were found, which was not surprising since Ag retention was very low (see Table 1). Generally, precipitates containing transuranic elements, i.e., U and Pu, were more prevalent in Location A, which was in the vicinity of the buffer/IPyC debonded region in the this TRISO particle. Cracks in the IPyC layers of the TRISO particles have been observed to be preferential accumulation areas for fission products and transuranics [11] and the gap in the buffer/IPyC layers in the vicinity of Location A may provide rapid transport to the SiC layer in this vicinity. Fission-product elements, i.e., Ag, Cd and Zr, were generally more prevalent in the SiC layer at Location B where the buffer/IPyC layer remained bonded.

The fission product precipitates in both Locations A and B were found to be mostly associated with random, high-angle grain boundaries as shown in Fig. 3b. Grain boundaries exhibiting CSL relationships contained ~20% of the precipitates while low-angle grain boundaries were found to be associated with very few precipitates. No influence of or correlation with location within SiC layer—i.e., inner center or outer regions—are apparent in Fig. 3b. These results are consistent with that reported for TRISO particles irradiated in the AGR-1 experiment and analyzed in a similar manner [2].

III.B. AGR2-223-RS06—Comparison of Grain Boundary Distributions in Locations A & B

The grain-boundary distributions in the SiC layer of this particle are shown in Fig. 4. All distributions associated with the two locations (A and B) are statistically the same. A major portion of grain boundaries exhibit CSL-related misorientations (~50%) while random, high-angle grain boundaries are next most-prevalent (~30%), with low-angle grain boundaries making up the remainder, at ~20%, Fig. 4c. In contrast to the results for AGR2-222-RS36, no large differences in the twin boundary fraction as a function of location or area within the SiC layer was found. However, for this particle, a slightly lower fraction of low-angle grain boundaries may exist at Location B compared to Location A, Fig. 4c, which is in contrast to the results for AGR2-222-RS36, shown in Fig. 2c.

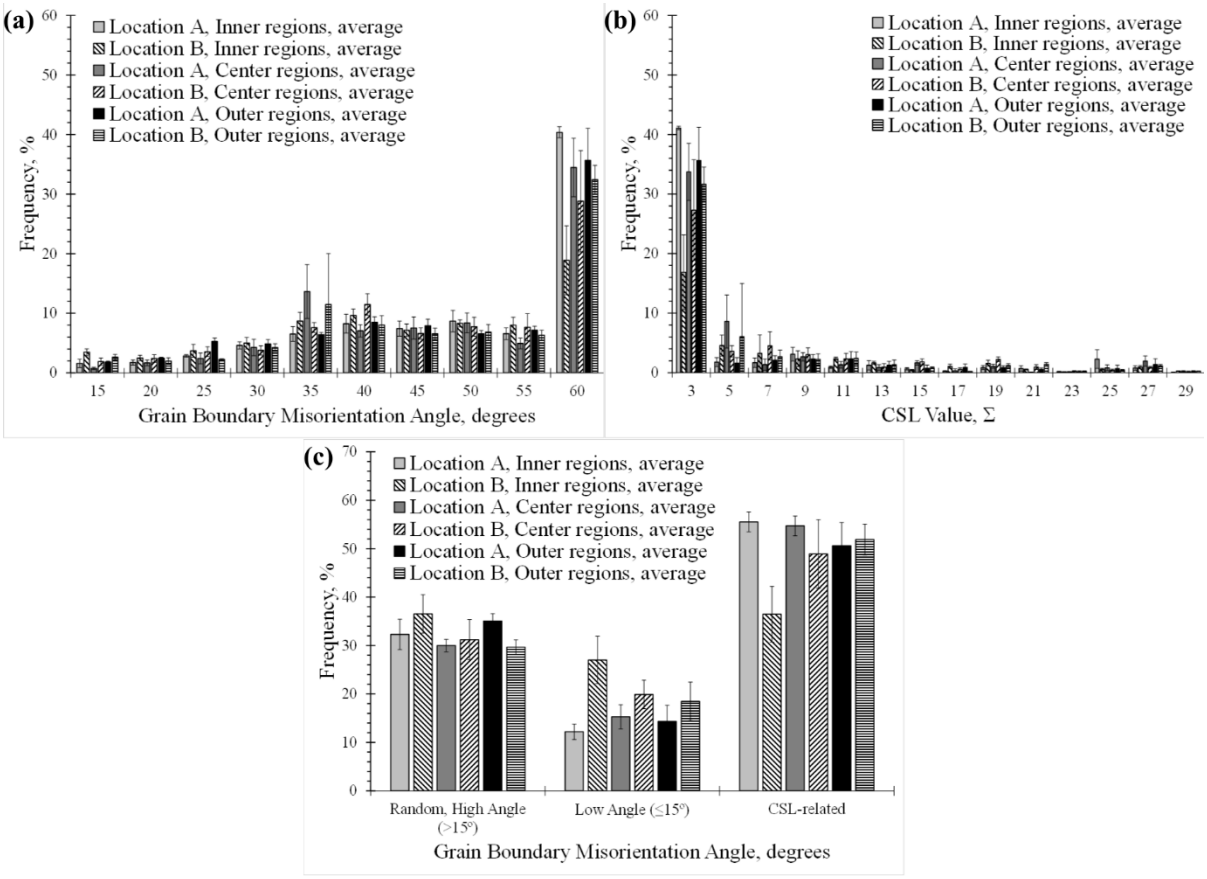

Fig. 2: Plots of various grain boundary characteristics as a function of position within the SiC layer at Locations A and B, AGR2-222-RS36.

The results of EDS analyses of the precipitates in the analyzed areas of the SiC layer are shown in Fig. 5a. Again, most of the precipitates contained Pd as the only fission product (grain boundary precipitates in the SiC layer may also contain Si and/or C [12], but was not definitely determined in this study because these elements are present in the surrounding SiC grains). As with the results for AGR2-222-RS36, the precipitates in Location A (in the vicinity of the buffer/IPyC debonded region) exhibited a wider variety of fission product elements and combinations of those elements than in Location B (Fig. 5a). Again, the buffer/IPyC debonded region is expected to provide a fast transport path, allowing fission-product elements to reach the SiC layer quicker than in areas where the buffer and IPyC layers remain bonded.

Most of the fission product precipitates were found to be associated with random, high-angle grain boundaries throughout the SiC layer at both Locations A and B, Fig. 5b, as was found for AGR2-222-RS36. Smaller fractions of fission-product precipitates were found to be associated with CSL-related grain boundaries. No precipitates were found associated with low-angle grain boundaries. These trends were statistically the same in all areas within the SiC layer—i.e., the inner, center, and outer areas—at both Locations A and B.

IV. DISCUSSION

Because the grain-boundary distributions at the inner, center, and outer regions in the SiC layer were statistically the same, with only a few, but potentially important exceptions (see Section IV.C, below), the grain-boundary data from inner, center and outer regions were combined to provide average grain-boundary distributions in the SiC layer at Locations A and B so that comparisons of the grain boundary distributions in each particle could be made more easily.

IV.A. Comparison of AGR2-222-RS36 & AGR2-223-RS06

Fig. 6 compares the average SiC grain boundary distributions between the two AGR-2 particles at

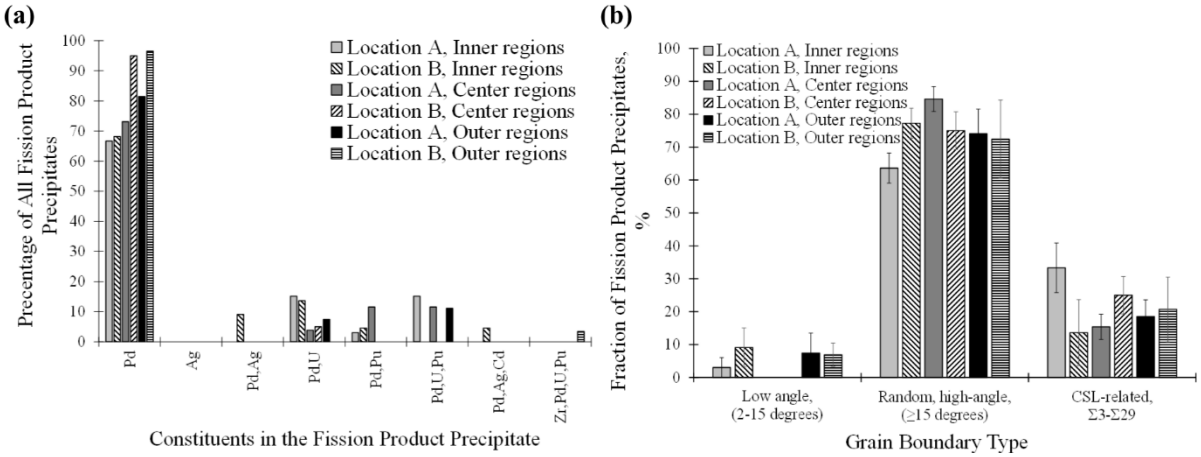

Fig. 3: Distribution of fission products by (a) composition and (b) grain boundary type, AGR2-222-RS36.

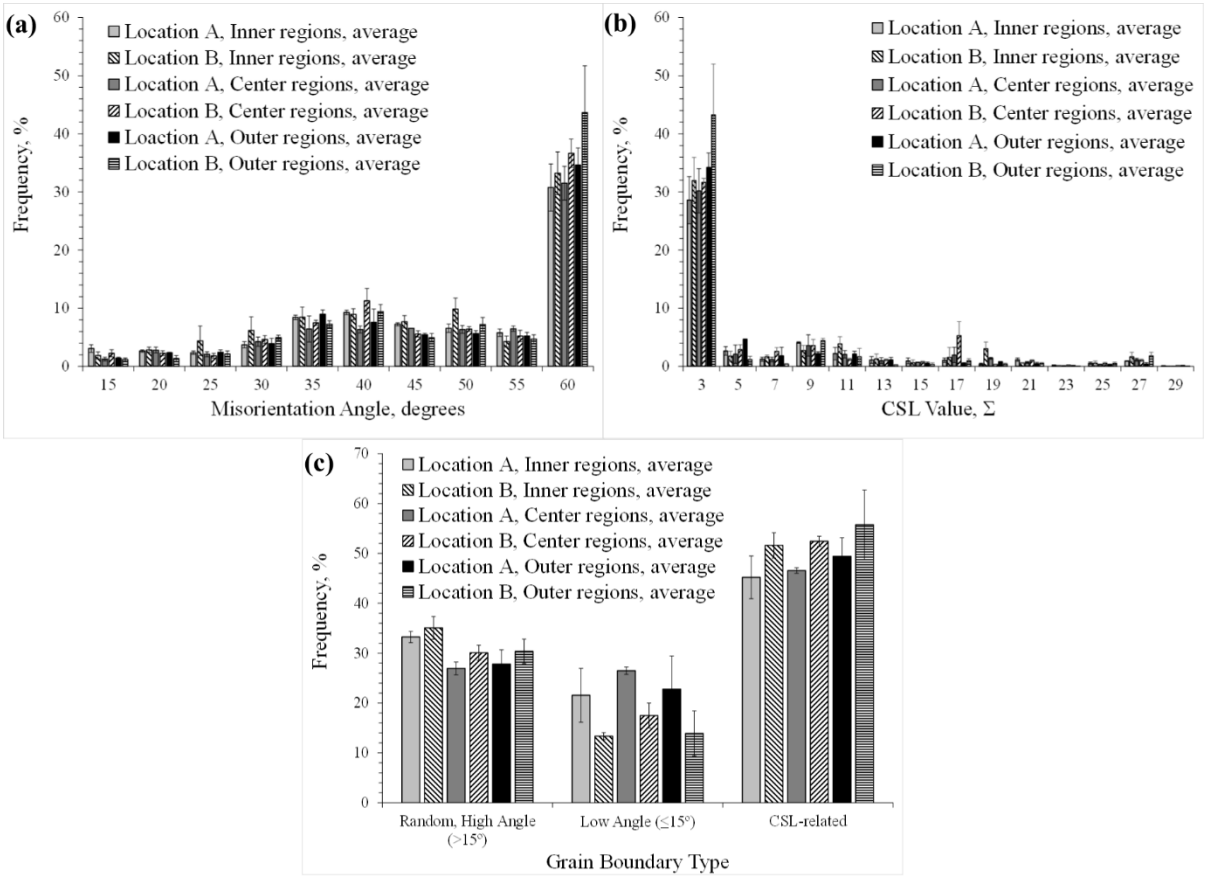

Fig. 4: Plots of various grain boundary characteristics as a function of position within the SiC layer at Locations A and B, AGR2-223-RS06.

Locations A and B (i.e., in and away from the vicinity of the buffer/IPyC debonded region), respectively. The grain boundary distributions at Location A in both particles are similar, with the only significant difference being the low-angle grain boundary fraction, which is higher in AGR2-223-RS06, Fig. 6c. At Location B, this trend is reversed, with AGR2-222-RS36 exhibiting a higher fraction of low-angle grain boundaries. Additionally, the twin fraction at Location B on AGR2-222-RS36 is lower than that found at Location B on AGR2-223-RS06, as well as on both particles in Location A, Fig. 6b. Since it is unlikely that the microstructure of the SiC layer could

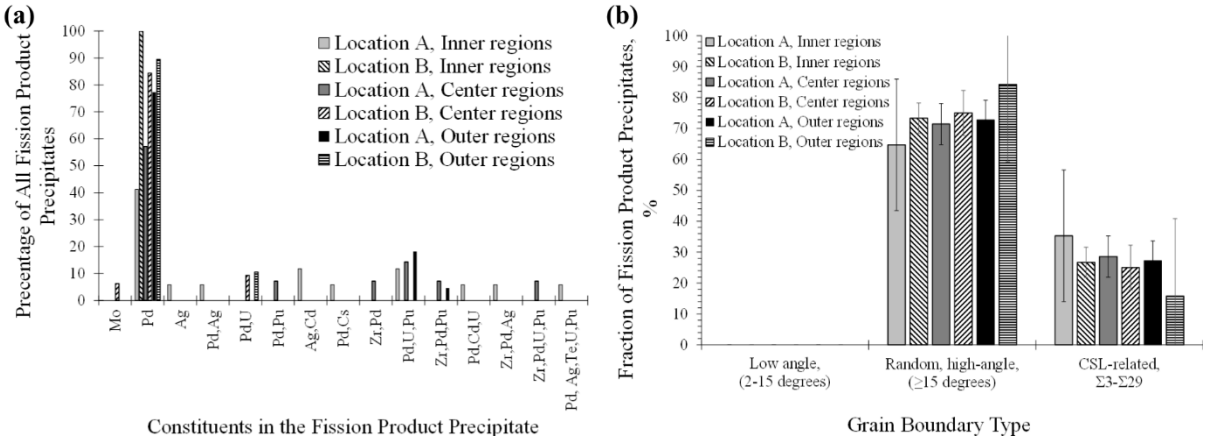

Fig. 5: Distribution of fission products by (a) composition and (b) grain boundary type, AGR2-223-RS06.

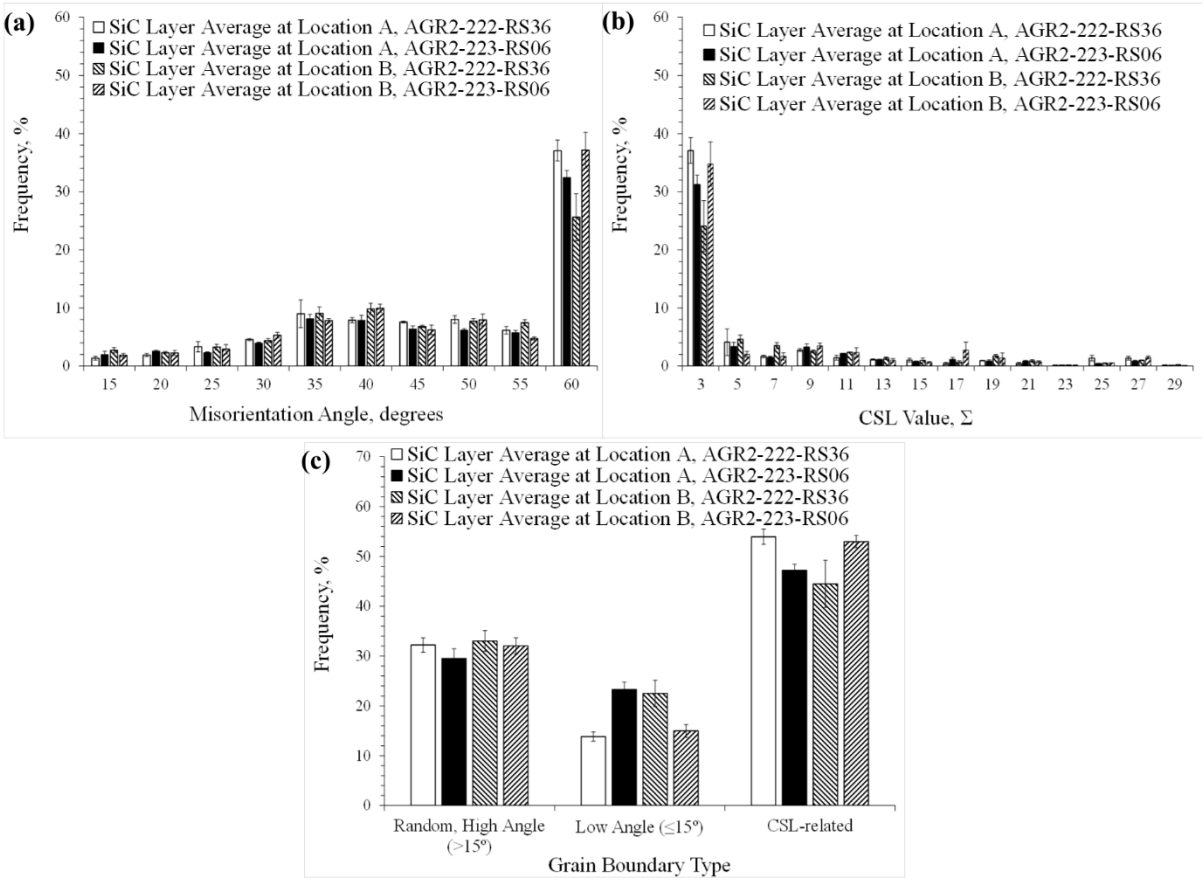

Fig. 6: Comparison of the grain boundary distributions in the vicinity of buffer/IPyC debonded regions (solid bars) and intact regions (hatched bars) for the two AGR-2 TRISO particles.

somehow influence the propensity for the buffer/IPyC interface to debond, these results imply that an inherent location-to-location, as well as particle-to-particle, variability of the grain-boundary distribution in the SiC layer arises during the fabrication of TRISO particles.

The correlation of fission-product precipitates with different types of grain boundaries in the two locations for both particles is shown in Fig. 7. The trends are independent of location on the particle. This is not surprising given the determining factor of precipitate formation is the grain boundary energy, as discussed in [2,13].

Overall, the differences in the average grain-

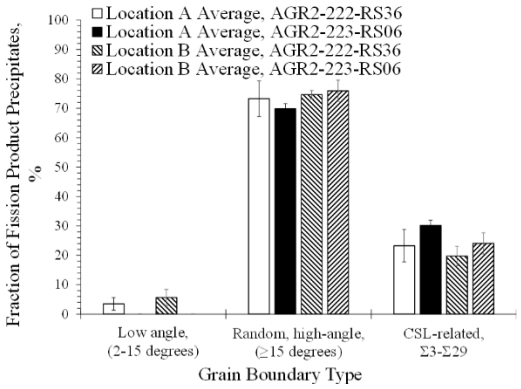

Fig. 7: Comparison of the fission product precipitate distribution in the vicinity of buffer/IPyC debonded regions (solid bars) and intact regions (hatched bars) for the two AGR-2 TRISO particles.

boundary distributions discussed here appear to be minor, as shown in Fig. 6, and whether they can have a significant influence on fission-product transport through the SiC layer will be discussed in more detail below.

IV.B. Comparison of AGR-2 and AGR-1 TRISO Particles

One of the prime objectives of the AGR-2 experiment was to demonstrate the performance and behavior of TRISO particles fabricated at pilot scale were the same as TRISO particles fabricated at laboratory scale, i.e., AGR-1 TRISO fuel. The AGR-2 TRISO fuel particles were fabricated using conditions very similar to those used to fabricate AGR-1, Variant 3 TRISO fuel particles; thus, a direct comparison of AGR-2 and AGR-1, Variant 3 irradiated TRISO particles is of interest to ensure up-scale in production has not introduced new characteristics in the SiC layer that adversely affect performance.

Fig. 8 plots the grain boundary distributions for Locations A and B on particles AGR2-222-RS36 and AGR2-223-RS06 with the distributions found for AGR-1, Variant 3 particles that have been previously analyzed with similar methods. (It should be kept in mind in the discussions that follow that AGR2-222-RS36, AGR1-433-01 and AGR1-433-04 were all safety tested at 1600°C while the other particles were not. Also, the neutron fluence, burnup and TAVA were similar, but not exactly the same, for each particle.) Overall, the plots in Fig. 8 show grain-boundary distributions are very similar. Two notable differences include the low twin fraction found in AGR2-222-RS36, at the arrow in the plots of Fig. 8, which was significantly lower than in any particle—AGR-1 or AGR-2—of the dataset. Also, the two AGR-2 particles seem to have locations with significantly smaller low-angle grain boundary fractions (Location A in AGR2-222-RS36 and Location B in AGR2-223-RS06) than the AGR-1 particles. Again, these variations appear to indicate inherent variation that arises, most likely, during fabrication. (Previous analyses on other variants of AGR-1 particles conclude that irradiation has little effect on the as-fabricated SiC microstructure [2].) However, it should again be noted that the actual individual particle temperature during irradiation is not known with certainty. The spatial temperature variation within the compact can be on the order of 300°C from the coldest part to the hottest part [10]. Thus some particles may have experience more thermally-driven creep than others.

IV.C. Influence of Local Grain Boundary Distribution on Ag-110m Retention

The SiC layer is the primary barrier to the transport of fission-products out of the particle, and the influence of microstructure on transport is of concern. While Ag-110m is not a concern for off-site dose consequence in gas-cooled reactors, it does readily transport through intact TRISO layers. Therefore, Ag-retention behavior was plotted as a function of the fraction of boundaries exhibiting specific grain-boundary characteristics, i.e., the random, high-angle fraction, and twin fraction, in Fig. 9, for areas in the inner, center, and outer regions of the SiC layer of the AGR-2 particles and the Variant 3, AGR-1 particles. Previously it was found, among AGR-1 particles of the baseline and Variant 1 variety, that a correlation existed between Ag-110m retention and both the random, high-angle fraction and the twin fraction in the SiC layer [2]. This correlation was most well-defined only in the center region of the SiC layer. The plots of Fig. 9 indicate a similar behavior. In the inner and outer regions, there appears to be little if any correlation between Ag-110m retention and either the random, high-angle grain boundary fraction or the twin (Σ3) fraction, Figs. 9, a and b and 9, e and f. However, the center areas of the SiC layer in the AGR-2 particles do seem to be consistent with a correlation between Ag-110m retention and both the random, high-angle and twin fractions exhibited by the AGR-1 particles, Fig. 9, c and d, although AGR-2 particles with higher Ag retention need to be studied to verify this observation. As discussed previously [2,13], random, high-angle grain boundaries are expected to aid in Ag transport due to their inherently high-impurity atom diffusivity - resulting in a positive correlation between particle Ag release and the high-angle grain boundary fraction. In contrast, twin

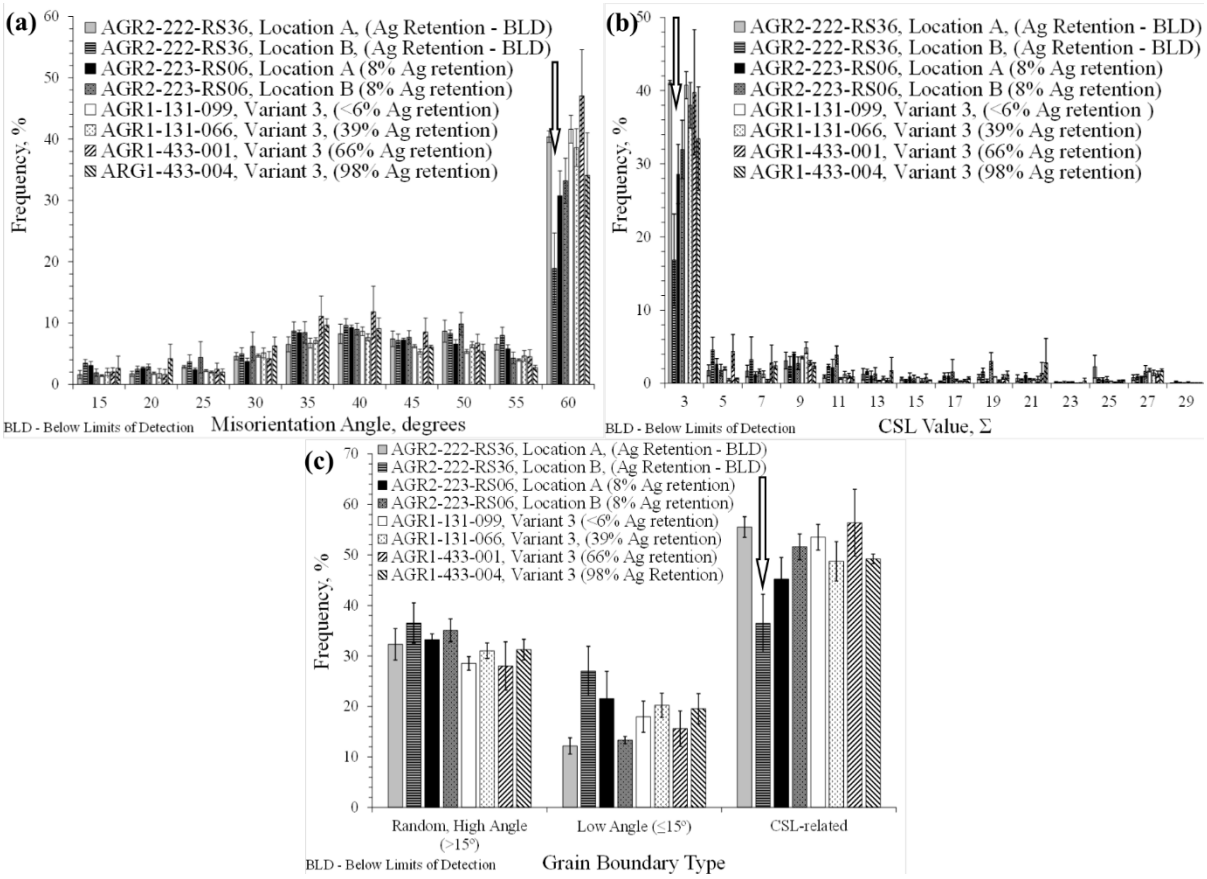

Fig. 8: Comparison of the SiC grain boundary distributions of AGR-1 and AGR-2 irradiated TRISO particles.

boundaries are expected to have poor Ag-transport properties and give rise to a negative correlation where less Ag release occurs when the twin boundary fraction is higher. These positive and negative correlation behaviors are exhibited by the AGR-1 particles, and supported by the AGR-2 data, in the plots of Fig. 9 c and d. In this center region, the growth of the CVD SiC layer is transitioning from nucleation to steady-state growth. This transition in microstructure is suggested by the random, high-angle and CSL-related grain-boundary fractions in Figs. 2c and 4c. In these plots, the random, high-angle fraction decreases from the inner areas to the outer areas of the SiC layer while the CSL-related fraction increases (although the error bars suggest these trends may not be significant).

Only the grains initially deposited with a fast-growth direction oriented in the radial direction survive while grains oriented with a slower growth rate are squeezed out during subsequent CVD deposition. The plots of Fig. 9 seem to suggest that this transition area is critical in determining the overall Ag-110m-transport behavior of the SiC layer. As mentioned, similar correlations in the center regions of the SiC layer are observed in AGR-1 particles of other variants.

V. SUMMARY AND CONCLUSIONS

The grain boundary distributions in the SiC layer of two TRISO particles irradiated during the AGR-2 experiment were characterized as a function of position within the SiC layer using precession electron diffraction techniques. Two locations on each particle were analyzed: one in the vicinity of a buffer/IPyC layer delamination and one far away from this delamination. Additionally, precipitates on grain boundaries were qualitatively analyzed for the presence of fission product elements and correlated with grain boundary type.

The following conclusions were made in this study:

- Grain boundary distributions in the vicinity if the buffer/IPyC delamination and far from it were essentially the same, with small differences in the low-angle grain boundary fractions and the twin fraction that were attributed to the inherent variability in the SiC layer produced by the CVD fabrication process.

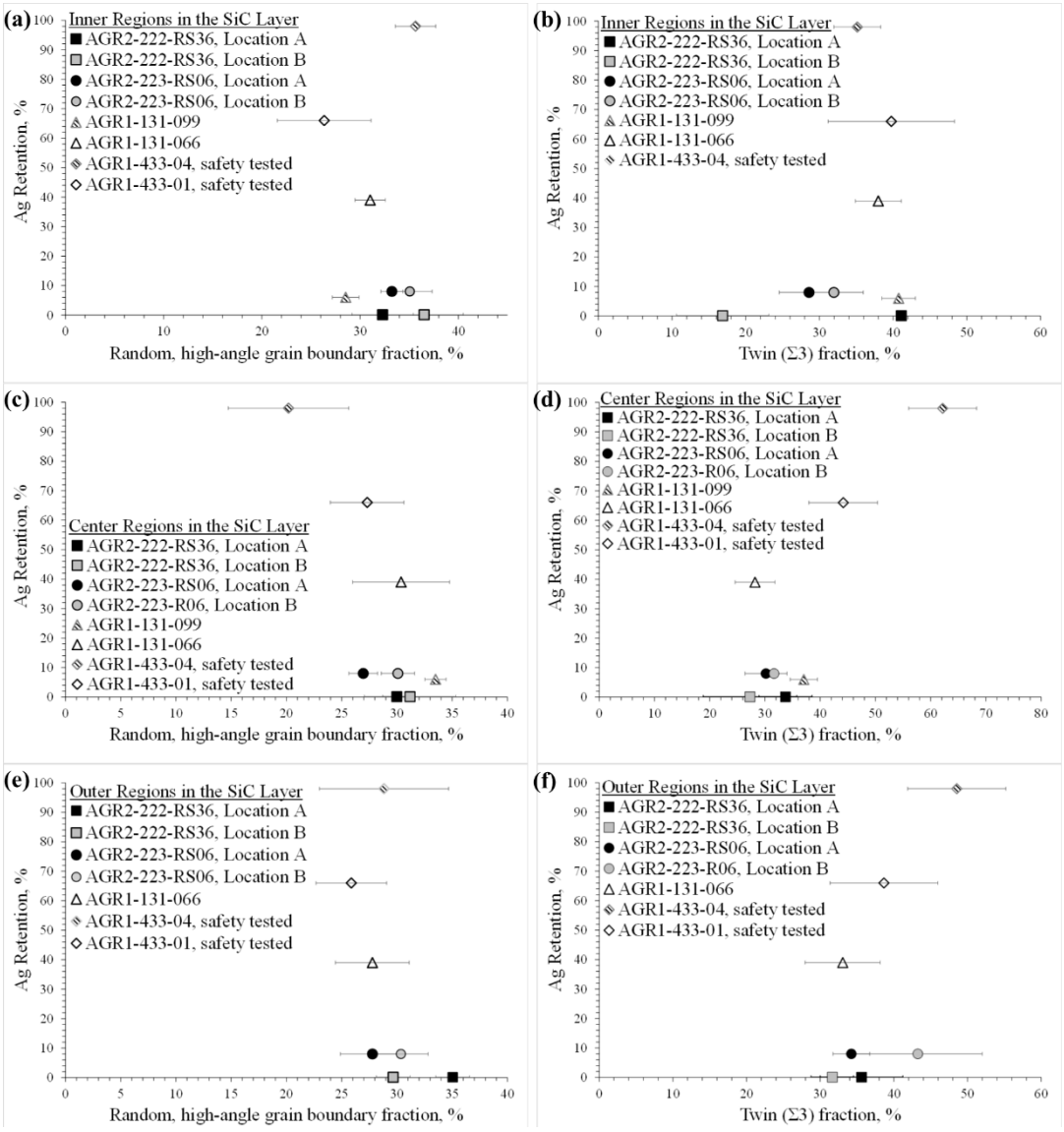

Fig. 9: Plots of Ag retention as a function of the random, high-angle grain boundary fraction (left column) and the twin boundary fraction (right column) for (a and b) inner, (c and d) center and outer (e and f) regions of the SiC layer.

- Pd was the fission-product element found most often in the precipitates, although a few precipitates containing Ag, Cd, Cs, Te, Zr and Mo (in various combinations) were also found.
- Most precipitates were associated with random, high-angle grain boundaries; although precipitates were found on grain boundaries with a CSL-relationship to a lesser degree, very few were found on low-angle grain boundaries.
- Locations in the vicinity of the buffer/IPyC debonded region tended to have precipitates exhibiting a greater variety of fission-product elements than locations where the buffer/IPyC remains bonded, suggesting the debond allowed fast transport of the fission-product elements to the SiC layer.
- Comparison of the results to previously irradiated and analyzed, Variant 3, AGR-1 TRISO particles showed the grain boundary distributions were similar. The grain boundary distributions in the AGR-2 particles were not consistently different from those of the AGR-1 particles, and it was concluded that differences were, again, inherent to the fabrication process.
- The grain boundary distributions in AGR-2 and AGR-1 particles were used to study Ag-110m retention versus the fraction of various grain-boundary parameters. Possible correlations

between high Ag-110m retention and low random, high-angle grain boundary fractions, as well as between high Ag-110m retention and high twin fractions, were found for the center regions of the SiC layer. Analysis of AGR-2 particles with higher retained Ag content is needed to confirm this observation in AGR-2. Ag-110m retention in the inner and outer areas of the SiC layer appeared to be independent of these grain-boundary fractions. Therefore, the correlation was attributed to the transition in microstructure in the center area that arises during the CVD fabrication process.

- Further study with an irradiated set of TRISO fuel particle—subjected to the same particle temperature history, burnup, and neutron fluence, along with microstructural evaluation techniques that can determine grain-boundary distributions for the entire SiC layer of each particle—are required to verify the correlations observed in this study.
- Overall, no major differences in the microstructure and irradiation behavior between pilot-scale AGR-2 particles and lab-scale AGR-1 TRISO particles were found.

VI. ACKNOWLEDGEMENTS

This work was sponsored under U.S. Department of Energy Idaho Operations Office Contract DE-AC07-05ID14517, as part of the Advanced Gas Reactor Development Program. Accordingly, the U.S. Government retains and the publisher, by accepting the article for publication, acknowledges that the U.S. Government retains a nonexclusive, paid-up, irrevocable, world-wide license to publish or reproduce the published form of this manuscript, or allow others to do so, for U.S. Government purposes.

REFERENCES

[1] I.J. van Rooyen, T. M. Lillo, H. Wen, K. E. Wright, J. Madden, and J. A. Aguiar, *Advanced Electron Microscopy and Micro-Analytical Technique Development and Application on Irradiated TRISO-Coated Particles from the AGR-1 Experiment*, INL/EXT-15-36281, January 2017.

[2] T.M. Lillo, I.J. van Rooyen, J.A. Aguiar, "Silicon carbide grain boundary distributions, irradiation conditions, and silver retention in irradiated AGR-1 TRISO fuel particles," *Nuc. Eng. Design* 329, 46-52 (2018).

[3] T.M. Lillo, I.J. van Rooyen, and Y.Q. Wu, "Precession Electron Diffraction for SiC Grain Boundary Characterization in Unirradiated TRISO Fuel," *Nuc. Eng. Design* 305, 277-283 (2016)

[4] R. Kirchhofer, J.D. Hunn, P.A. Demlowicz, J.I. Cole, B.P. Gorman, "Microstructure of TRISO coated particles from the AGR-1 experiment: SiC grain size and grain boundary character," *J. Nuc. Mater.* 432, 127-134 (2013).

[5] T.J. Gerczak, J.D. Hunn, R.A. Lowden, T.R. Allen, "SiC layer microstructure in AGR-1 and AGR-2 TRISO fuel particles and the influence of its variation on the effective diffusion of key fission products," *J.Nuc. Mater.*, 480, 257-270 (2016).

[6] C.M. Barnes, D.W. Marshall, J. Hunn, B.L. Tomlin, J.T. Keeley, "Results of tests to demonstrate a six-inch diameter coater for production of TRISO coated particles for advanced gas reactor experiments," in: *Proceeding of HTR 2008, Washington D.C., United States, September 28-October 1, 2008.*

[7] B.P. Collin, *AGR-2 Irradiation Test Final As-Run Report*, INL/EXT-14-32277, rev. 2, August 2014.

[8] Sterbentz, J.W., "JMOCUP As-Run Daily Depletion Calculation for the AGR-2 Experiment in ATR B-12 Position", ECAR-2066, Idaho National Laboratory, 2014.

[9] ASTM Standard E2627-13, "Standard Practice for Determining Average Grain Size Using Electron Backscatter Diffraction (EBSD) in Fully Recrystallized Polycrystalline Materials.", ASTM International, West Conshohocken, PA, 2013, www.astm.org.

[10] G.L. Hawkes and P.E. Murray, "AGR-1 Daily As-run Thermal Analyses," Idaho National Laboratory, ECAR-968 rev 4, INL/MIS-11-23668, 2014.

[11] H. Wen, I.J. van Rooyen, J.D. Hunn, T.J. Gerczak, "Electron Microscopy Study of Pd, Ag, and Cs in Carbon Areas in the Locally Corroded SiC Layer in a Neutron-Irradiated TRISO Fuel Particle," *J. of the European Ceram. Soc.* (2010), https://doi.org/10.1016/j.jeurceramsoc.2018.05.003

[12] E.J. Olivier and J.H. Neethling, "The role of Pd in the transport of Ag in SiC," *J. Nucl. Mater.*, 432, 252-260 (2013).

[13] T.M. Lillo and I.J. van Rooyen, "Influence of SiC grain boundary character on fission product transport in irradiated TRISO fuel," *J. Nuc. Mater.* 473, 83-92 (2016).